

20 IMPROVING NEURAL NETWORKS TRAINED WITH LIMITED DATA BY
21 DERIVING IMPROVEMENTS BASED ON KNOWLEDGE OF THE UNDERLYING
22 PHYSICS INTERACTIONS

23 by

24 Jose G. Perez

25 THESIS PROPOSAL

26 Presented to the Faculty of the Graduate School of

27 The University of Texas at El Paso

28 in Partial Fulfillment

29 of the Requirements

30 for the Degree of

31 DOCTOR OF PHILOSOPHY

32 Department of Computer Science

33 THE UNIVERSITY OF TEXAS AT EL PASO

34 January 20, 2025

Table of Contents

35

	Page
36	
37	Table of Contents iii
38	Abstract v
39	1 Introduction vi
40	1.1 The Need For Data In Neural Networks vi
41	1.2 The Difficulty of Getting Data vi
42	1.3 Working Around Data Limitations With Few-Shot Learning vii
43	1.3.1 Transfer Learning viii
44	1.3.2 Data Augmentation ix
45	1.3.3 Meta Learning ix
46	1.4 Few-Shot Learning By Integrating Physics Into Neural Networks xi
47	1.5 Specific Problems From Other Disciplines That Have Limited Datasets xii
48	1.5.1 Fluid Flow Velocity Prediction xii
49	1.5.2 Glacial Ice Segmentation xv
50	1.6 Thesis Statement xvii
51	1.7 Expected Contributions xviii
52	2 Physics-Informed LSTM Network For Velocity Prediction of Fluid Flow Simulations xx
53	2.1 The Importance of Fluid Flow Velocity Prediction xx
54	2.2 Long Short-Term Memory Networks (LSTMs) For Time Series Data xxi
55	2.3 Adding Physics to LSTMs xxii
56	2.3.1 Fluid Flow Velocity Data From Simulations xxiii
57	2.3.2 Measuring Network Performance With The Mean Squared Error xxv
58	2.3.3 Proposed Network Architecture xxvi
59	2.3.4 Baseline Used To Compare Against Our Proposed Network xxix
60	2.3.5 Experimental Results xxix

61	2.3.6	Conclusion	xxx
62	3	Glacial Ice Segmentation of the HKH Region With Physics-Informed Data Aug-	
63		mentation	xxxix
64	3.1	The Importance of Glacial Ice Segmentation	xxxix
65	3.2	Image Semantic Segmentation: Grouping Similar Pixels Together	xxxix
66	3.3	Glacier Mapping Through Segmentation of Ice in Hyperspectral Images . .	xxxix
67	3.4	Convolutional Neural Networks: The Backbone of Almost All Networks That	
68		Use Images	xxxix
69	3.5	UNet: The Standard Network For Image Segmentation	xxxix
70	3.5.1	Measuring Network Performance With IoU	xxxix
71	3.6	Adding Physics To Image Segmentation Through Data Augmentation . . .	xxxix
72	3.6.1	Glacier Mapping Data From ICIMOD And Landsat7 Satellite . . .	xli
73	3.6.2	Baseline Network	xli
74	3.6.3	Experimental Results	xli
75	3.6.4	Conclusion	xli
76	4	Physics-Informed Network For Glacial Ice Velocity Predictions	xliii
77	5	Physics-Informed MANet for Glacial Ice Segmentation of the HKH Region . . .	xliii

Abstract

78

79 Deep neural network models are state-of-the-art for many image, audio, text, and video
80 processing problems in different fields of study and disciplines. However, training many of
81 these networks can require a lot of data and gathering such data can be time consuming,
82 costly, and difficult to set-up. This limiting factor can prevent researchers and engineers
83 that do not have access to a lot of resources from using all the tools and models available
84 in deep learning to tackle novel problems in their respective fields. To work around these
85 data limitations, many techniques and models in the field of Few-Shot Learning have been
86 proposed over the years in the sub-fields of transfer learning, data augmentation, and meta
87 learning. One such model, Physics-Informed Neural Networks or PINNs, relies on the fact
88 that datasets collected in the real world must follow the laws of physics, allowing us to
89 leverage our knowledge of physics to help improve performance on these datasets without
90 requiring more data to be gathered. I propose 4 ways of extending this type of approach that
91 leverages our knowledge of physics through new models and data augmentation techniques
92 in this dissertation, and apply these approaches to two problems that have limited datasets:
93 the problem of Fluid Flow Velocity Prediction in the field of mechanical engineering and
94 the problem of Glacial Ice Segmentation from geology.

95 A detailed explanation of the importance of data gathering, difficulties and limitations,
96 and my expected contributions for this area along with a timeline are presented in Chapter
97 1. The remaining chapters each describe one of the four expected contributions of my
98 dissertation in chronological order.

Chapter 1

99

Introduction

100

1.1 The Need For Data In Neural Networks

101

102 Deep neural network models dominate as the state-of-the-art machine learning (ML) models
103 that have the best performance across many different image [1] [2] [3], text [4], and video
104 processing tasks applied to multiple disciplines and fields of study. From text generation
105 with large language models (LLMs) such as GPT-3 [5], object tracking used by the space
106 sector to analyze the sun [6] and other galactic bodies, object detection used by self-driving
107 cars [7], to the rise of mobile apps for synthetic audio and image generation that has caught
108 the attention of regular everyday people. Although there are different architectures and
109 different ways to train these networks depending on the task being considered, there is a
110 big commonality among all machine learning (ML) models which is the need to have a lot
111 of data to train these models.

1.2 The Difficulty of Getting Data

112

113 Data gathering is one of the most fundamental and important problems in machine learning
114 (ML), as without data there is nothing to train your models with and the quality and
115 quantity of your data makes a big impact on the performance of your given model. The
116 state-of-the-art text generation model GPT-3 [5] was trained on 45TB of text data crawled
117 from the publicly available Internet, Google trained their MLP-Mixer [8] and a few other
118 models a 300 million image private subset of the images extracted from their search engine
119 database called JFT-300M, and NVIDIA's StyleGan2 [9] research used the FFHQ dataset

120 which has 70,000 images and the LSUN dataset which has 10 categories with each having
121 from 120,000 to 3,000,000 images.

122 Although there have been efforts made in different fields to create uniform and useful
123 datasets, data gathering is still one of the main limiting factors preventing researchers of
124 other disciplines from using all the tools and models we have available in deep learning.
125 Data gathering is typically very time consuming, difficult to set-up, and costly in terms
126 of monetary expenses. Big tech companies don't struggle with this problem as much as
127 university researchers and smaller companies do as they have bigger budgets and more
128 staff available for data collection purposes. Even though the research groups as these
129 companies sometimes make their datasets publicly available for others to use [10] [11]
130 [12], these datasets which usually consist of RGB photographs are not useful to people in
131 other fields of study to solve problems in their respective disciplines. The data needed to
132 solve problems in neuroscience, geology, medicine, and other disciplines will often require
133 advanced equipment, domain experts, and be stored in a different digital format than
134 regular camera photographs.

135 **1.3 Working Around Data Limitations With Few-Shot** 136 **Learning**

137 The challenges of data gathering and the eagerness of researchers to use neural networks
138 has steadily given rise to a field called "Few-Shot Learning" over the years. The idea
139 behind few-shot learning is to train deep neural network models with a "few" labeled
140 data samples but still achieve good performance for the given problem. This way you
141 can leverage as much power from these deep neural networks that you can with as little
142 data as possible, making deep neural networks more accessible. Proposed few-shot learning
143 approaches typically focus on taking one component of the traditional deep neural network
144 training pipeline and adapting it to perform better with few training samples. There are

145 3 main types of approaches, and although I present these approaches as separate fields in
146 the area of “few-shot learning” it is not uncommon to have one approach from each field
147 as part of your final model.

148 1. **Transfer Learning** - Approaches where you take pre-trained models trained on
149 large datasets for a similar problem to yours and then “transfer” some of the learned
150 knowledge to your limited data problem.

151 2. **Data Augmentation** - Approaches that propose ways to generate more data samples
152 from your existing ones to increase your dataset size.

153 3. **Meta Learning** - Approaches where your network “learns to learn” or extracts some
154 useful knowledge on how to train your network for your problem by training other
155 networks on subsets of other similar data and similar problems in what is called
156 “episodic training”.

157 **1.3.1 Transfer Learning**

158 In transfer learning the goal is to take models that are already trained and then “transfer”
159 as much useful knowledge as possible to your specific problem. This is done by simply
160 loading a trained network, freezing some of the layers so they do not get updated while
161 training anymore, removing the last layer which is usually problem dependent, and adding
162 a last layer that fits your specific problem.

163 However, this only works well when the network is pre-trained on data that is similar
164 to yours. The bigger the gap between the domains and problems used for the pre-trained
165 network and your own, the worst the performance will be with transfer learning. Because
166 of this big problem, the cases where you can actually use transfer learning and get good
167 results are few unless you are working with RGB images for the common tasks of object
168 classification or detection. If you are using a different type of input data for a different
169 task, the odds that you will find a pre-trained model with similar data to yours becomes
170 much lower.

171 **1.3.2 Data Augmentation**

172 In data augmentation the goal is to take your existing limited data and generate “new”
173 samples from them to increase the size of your dataset. If you have image data, one of the
174 simplest and most popular approaches is to perform simple image processing operations like
175 rotation, cropping, re-sizing, mirroring, and more. However, this requires careful thinking
176 as not all operations will produce good augmentations. For example, for the MNIST [13]
177 hand-written digit dataset it does not make sense to flip or mirror images as the new images
178 will not represent the same digit as the original (a flipped 6 can become a 9). This is one
179 of the disadvantages of data augmentation, the augmentation must still represent the same
180 label as the original data so if your data is not based on images or is complex it may be
181 difficult to come up with rules for data augmentation.

182 **1.3.3 Meta Learning**

183 In meta-learning the goal is to extract useful information that can be used to train your
184 model by training other models and learning how and what those models learned (meta-
185 data). For example, let’s take the random initialization of networks. Although you can
186 use a uniform or normal distribution, MAML [14] proposes learning an initialization that
187 leads to maximal performance on a new problem with a few training steps and a small
188 amount of data. This is done by feeding entire “problems” as input data and optimizing
189 the model to produce good results with as few training steps as possible. Therefore you
190 train this model on other problems, and then you feed your specific problem to it so you
191 can also produce good results with few training steps. The drawback of this approach is
192 that it can be computationally expensive to train “entire problems” multiple times while
193 optimizing this architecture, the problem of vanishing/exploding gradients is still present
194 in this network, and selecting which extra problems and datasets to use can be a problem
195 as well.

196 Another popular meta-learning approach is called metric learning. The idea is pretty

197 simple, you might only have a few pictures of zebras and a few pictures of dogs so to classify
198 a new picture you can just compare it to a few of each and find which is the most similar.
199 Thus the main principle is to train models that can compute similarities through metrics.
200 Siamese Networks [15] are one of the earliest few-shot learning methods proposed to tackle
201 the limited data problem and this approach focuses on metric learning. Siamese Networks
202 take three inputs, a sample from your dataset called an anchor, a sample similar to your
203 anchor called the positive sample, and a sample different to your anchor called a negative
204 sample. Then the network is trained to produce embeddings (1D vectors) such that similar
205 samples are close in that metric space and different samples are further apart, allowing
206 you to use Euclidean distance to find similar samples. This idea was further improved in
207 Prototypical Networks [16], where the idea is now to find “prototypes” or samples that
208 represent a general class of similar objects instead of having the triplets. For example, you
209 may find one of your pictures is a good representation of “mammals” and can make it easier
210 to identify new mammals in the future. In Relation Networks [17] this metric learning idea
211 is generalized even more. Specifically, the authors propose an end-to-end two-part network
212 that is trained to learn a custom distance metric used to compare pairs of images called a
213 “relation score” instead of always using Euclidean distance. Then when a new image needs
214 to be classified, we can compare it against our few labeled samples and find the most similar
215 one or the one with the highest “relation score”. As the distance metric used for comparison
216 is custom learned, the model performs better than if you used general distance metrics like
217 Euclidean distance or Cosine similarity like in [16] or [15]. These type of architectures,
218 however, are typically designed for image classification problems and cannot be used as-is
219 for more complex tasks like image segmentation or object detection or for other types of
220 input data that are not regular camera RGB images.

1.4 Few-Shot Learning By Integrating Physics Into Neural Networks

One of the reasons why humans might be able learn new things with few examples and do few-shot learning is because we have a lot of previous knowledge that we leverage in our learning process and we never truly start from scratch as deep neural networks do. My research focus is then on how we can integrate our knowledge of physics to improve neural network performance and have models more “easily learn” with few examples, mimicking humans. Physics is a widely studied area of science that has been researched for hundreds of years for which we not only have a lot of mathematical equations but also a lot of expertise and knowledge in the field. As many problems across different disciplines are based on real-world data they must follow the “laws of physics” and so we can leverage our knowledge of physics to help improve performance on limited datasets that deal with real world data.

There exists an area of study called Physics-Informed Neural Networks (PINNs) [18] where the aim is to integrate physics that can be described as systems of partial differential equations (PDEs) directly into the loss function of a network. Unless you are working with simulation data, it will be close to impossible to collect all the variables and data needed to describe how your specific problem behaves exactly at all times. There is just too much data at too many different scales, from quantum effects all the way to space-time gravitational influences. Due to this, scales and times are often discretized when working with these PDEs like when using the Finite Element Method (FEM) to compute solutions for these PDEs. PINNs allow you to model some of these intrinsic variables of your data and use them along with the laws of physics (PDEs) that describe how they interact to increase your model performance. I will be extending this area by creating new network models and loss functions that will allow us to integrate PINNS and other neural network models to solve problems from two disciplines that have limited datasets.

247 **1.5 Specific Problems From Other Disciplines That** 248 **Have Limited Datasets**

249 As my research focus is on applying physics to neural networks to improve model perfor-
250 mance on problems with limited datasets I selected problems from two disciplines that had
251 limited data available and whose data must follow the “laws of physics” in some way. Those
252 problems were “Fluid Flow Velocity Prediction” from mechanical engineering and “Glacial
253 Ice Segmentation” from geology.

254 **1.5.1 Fluid Flow Velocity Prediction**

255 Understanding how fluids flow is very important for the study and development of airplanes,
256 cars, boats, rockets, and much more. One of the widely researched approaches used to study
257 fluid flow is setting up Computational Fluid Dynamic (CFD) simulations using software
258 developed specifically for that purpose like Ansys Fluent[19]. It is unfeasible to model every
259 particle of every fluid we are interested in modeling at every scale and every point in space
260 due to computational and time limitations, so it is necessary to define a discretized mesh
261 of finite elements of specific size as shown in Figure 1.1 below.

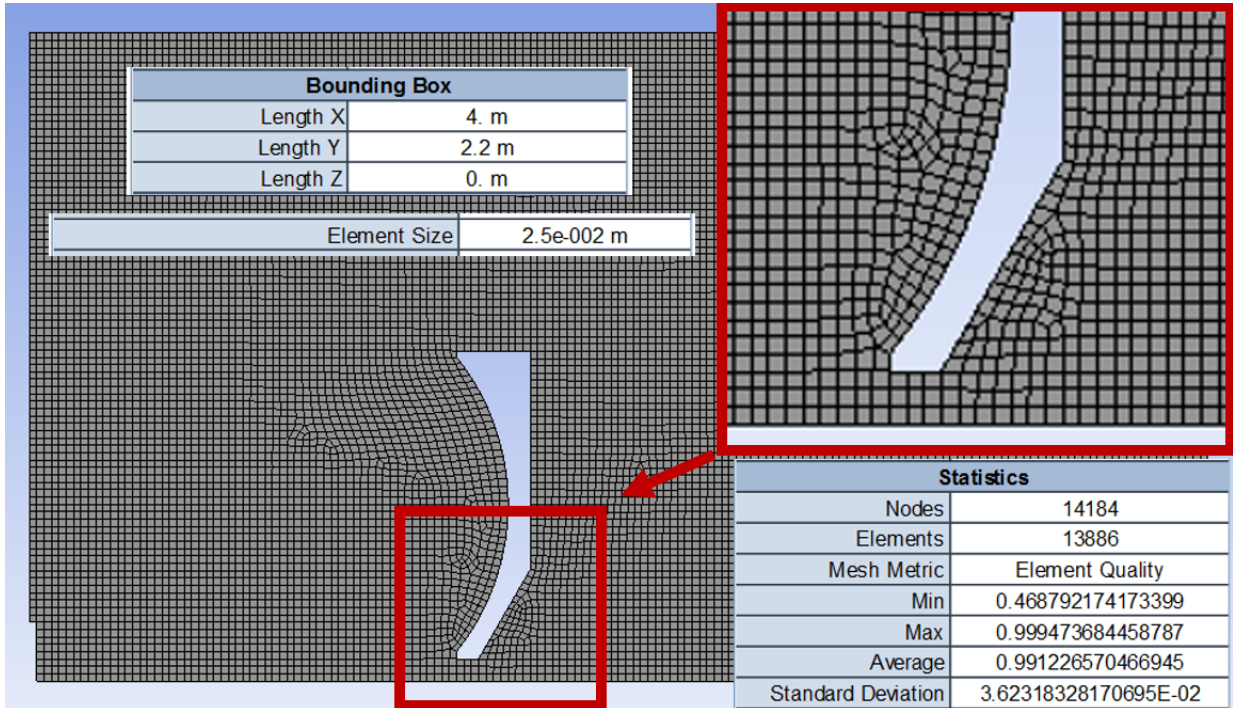


Figure 1.1: Example of a discretized mesh of finite elements used for a CFD fluid flow simulation.

262 After deciding the scale which we are interested in modeling and studying, the next
 263 step is to define the relevant geometry, fluids, and boundary conditions for the simulation
 264 as show in Figures 1.2 and 1.3 below. Lastly, a solver is selected and the simulation is run
 265 for a specific period of time.

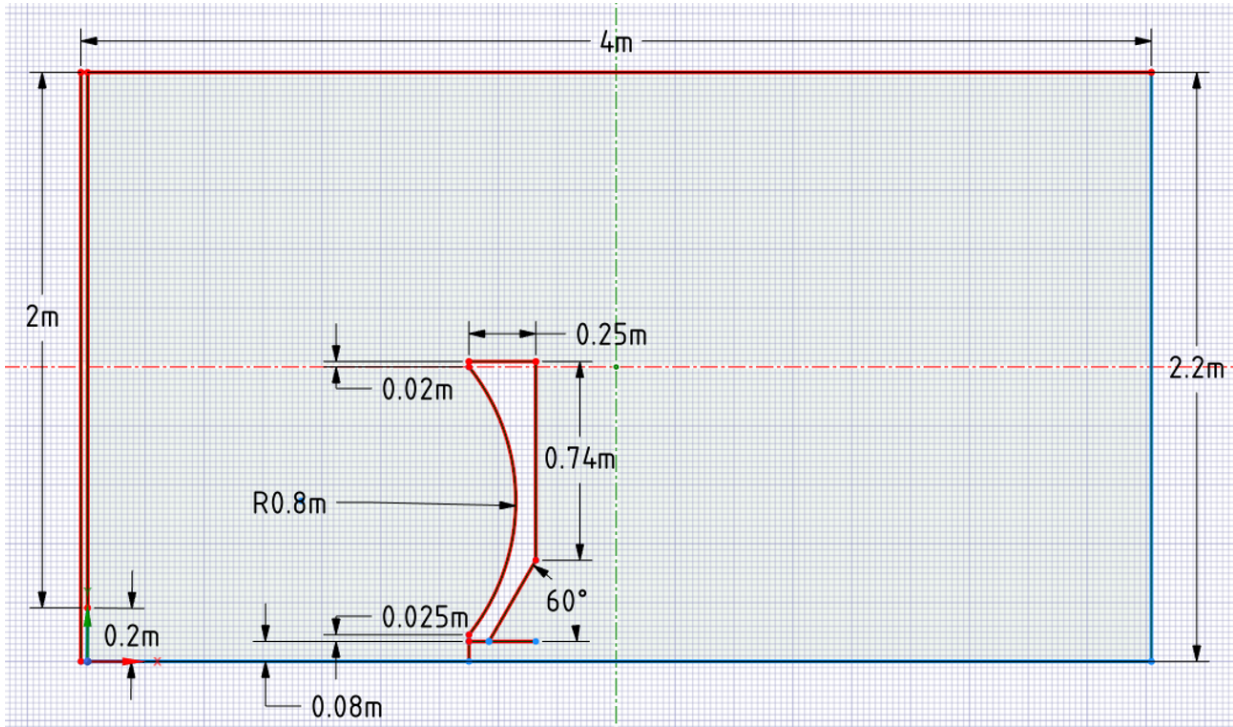


Figure 1.2: Example of geometry used for a CFD fluid flow simulation. This modeled geometry is for a proposed water-braking mechanism for a pusher sled system used in the Holloman Air Force Base for experiments.

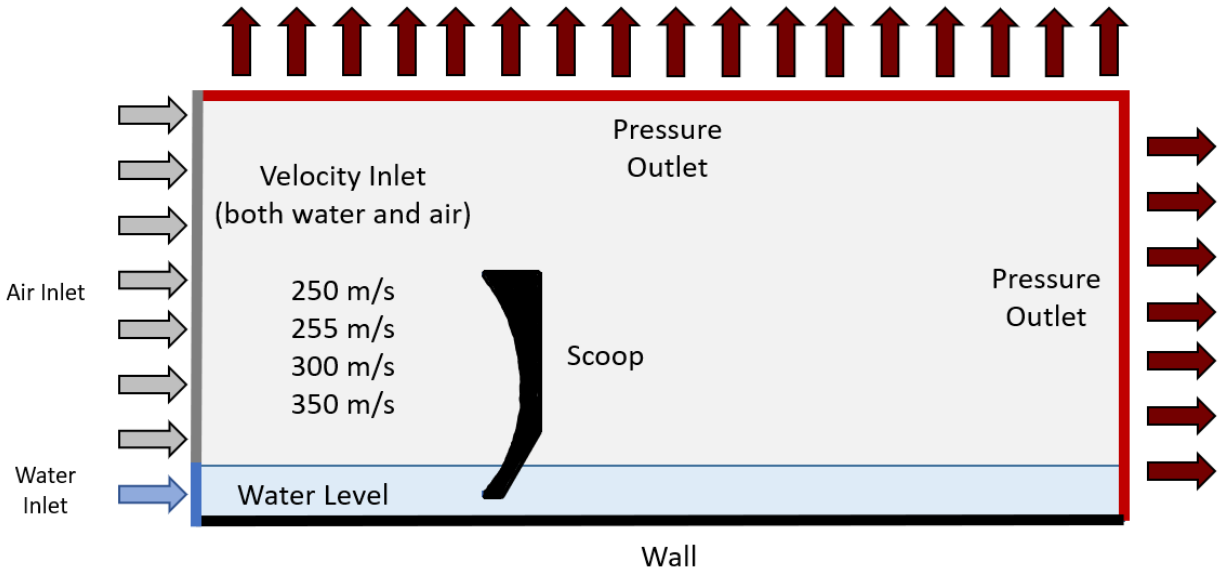


Figure 1.3: Example of boundary conditions used for a CFD fluid flow simulation. These boundary conditions model how the geometry (water-breaking scoop) will interact with the water as the pusher sled mechanism pushes the scoop at specific initial velocities.

266 One drawback of CFD simulations is that high-fidelity simulations can be very com-
 267 putationally expensive as having smaller finite elements, bigger meshes, bigger geometries,
 268 and bigger simulation environments increases the computations needed for the solvers to
 269 simulate each given time-step of the simulation. Although fluid flow datasets are available
 270 for some problems in fluid dynamics, many researchers are interested in fluid flows for spe-
 271 cific problems with different geometries and boundary conditions than those in the available
 272 datasets. As fluid flows are a widely studied area in mechanical engineering in the field of
 273 fluid dynamics, we know that the Navier-Stokes equations can be used to describe some of
 274 these flows and that these equations are partial differential equations (PDEs) allowing us
 275 to leverage Physics-Informed Neural Networks [18] to tackle this limited data problem.

276 1.5.2 Glacial Ice Segmentation

277 Glaciers are a very important source of water for people and wildlife of many different
 278 regions of the world, as not only do they provide a source of drinking water but also water

279 for watering crops and generating hydroelectric power [20]. As these regions rely heavily
280 on glacial melt as a water source, it is important to monitor and keep track of changes that
281 happen to these glaciers over time.

282 There exists multiple satellites such as NASA's Landsat-7, Landsat-8, and Sentinel-
283 2 that have captured hyperspectral images of these glaciers over a long period of time,
284 allowing glaciologists to take these images and use their expertise to determine what areas
285 of the images are clean ice, debris covered ice (ice mixed with rocks), and regular rocks in
286 a process called glacier mapping. This is one of the ways that these scientists monitor the
287 glaciers over time, and in the area of computer vision is called image segmentation. An
288 example of this is given in Figure 1.4 below.

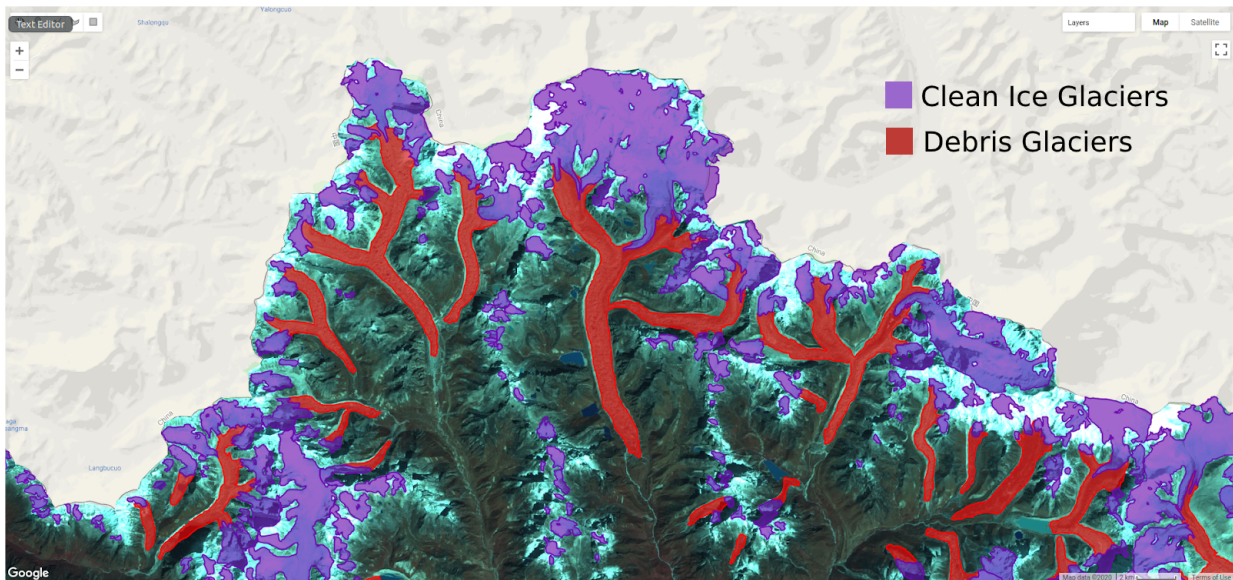


Figure 1.4: Example of glacier mapping or segmentation of a satellite image into clean ice and debris covered ice glaciers.

289 However, manually labelling hyperspectral satellite images into clean ice and debris
290 covered ice glaciers is a very time consuming task. This is due to two main reasons:

- 291 • Satellite images have more channels than the regular 3 (RGB) in digital cameras, so
292 they are hyperspectral images and require the usage of specialized tools (like QGIS)

293 and knowledge about what channels capture which bands of the electromagnetic
294 spectrum to properly visualize and analyze.

295 • High resolution images are difficult to segment as there are too many individual pixels,
296 and although glaciologists use tools such as QGIS to label the images using geometric
297 shapes instead of pixel by pixel to speed up the process it is still time consuming and
298 difficult to label the borders/boundaries between the clean ice and debris covered ice
299 specifically due to the amount of fine detail and care needed.

300 Labeling a single patch of a glacier using Sentinel-2 satellite imagery can take an expert
301 1 to 4 weeks depending on the complexity of the image, and the Hindu-Kush Himalayas
302 (HKH) glaciers are made up of at least 256 of such patches.

303 A labeled dataset exists for the glaciers in Hindu-Kush Himalayas (HKH) region created
304 by the International Centre for Integrated Mountain Development (ICIMOD) for images
305 taken with NASA’s Landsat-7 satellite. These images contain 7 channels including RGB,
306 Near-Infrared, and Digital Elevation Map data.

307 There also exists a dataset of glacier ice velocities created by the National Snow and Ice
308 Data Center containing the surface velocities of major glacier-covered regions in the world
309 including the Hindu-Kush Himalayas (HKH) spanning from 1985 to 2018 and compiled
310 from multiple of NASA’s Landsat satellites called the “MEaSURES ITS.LIVE Regional
311 Glacier and Ice Sheet Surface Velocities” dataset. As glacial ice velocity prediction is a
312 specialized form of fluid velocity prediction where the fluid being analyzed is ice from the
313 glaciers, we can use the Navier-Stokes equations once again to leverage Physics-Informed
314 Neural Networks [18] to help us tackle this limited data problem.

315 1.6 Thesis Statement

316 Incorporating physics in neural network models through modification of data and loss
317 functions will allow for better performance and faster convergence for the problems of fluid

318 flow velocity prediction and glacial ice segmentation.

319 **1.7 Expected Contributions**

320 The proposed contributions of this research are as follows:

- 321 **1. A physics-informed neural network model for the task of fluid flow velocity**
322 **prediction** - We will develop a model that uses Physics-Informed Neural Networks
323 (PINNs) [18] for the task of fluid flow velocity prediction and investigate ways to
324 combine PINNs with networks built for sequential data (such as [21]) to take advan-
325 tage of how fluid flows over time sequentially allowing for improvements on network
326 convergence speed.

- 327 **2. A neural network model with physics-informed data augmentation for the**
328 **task of glacier mapping** - As there already exists a network for glacier mapping by
329 image segmentation [22], we will investigate ways to augment the current available
330 labeled data for glacier mapping based on physics, improving the performance of the
331 pre-existing segmentation model.

- 332 **3. A physics-informed neural network model for the task of glacial ice velocity**
333 **predictions** - Glacial ice velocity prediction is a subset of the general fluid flow
334 velocity prediction problem, allowing us to use Physics-Informed Neural Networks
335 (PINNs) [18] combined with networks built for sequential data (such as [21] and [23])
336 to leverage the fact that glacial ice flows over time (sequentially) for the task of glacial
337 ice velocity prediction.

- 338 **4. A physics-informed neural network model for the task of glacier mapping**
339 - We will develop a new model based on a combination of Physics-Informed Neural
340 Networks (PINNs) [18] and a pre-existing segmentation model [22] for the task of
341 glacier mapping by segmenting glacier ice in satellite images. We will investigate ways

342 to combine datasets containing hyperspectral satellite images that have no velocity
343 information and datasets of ice glacier velocities to leverage the knowledge we have
344 about the physics of ice glacier velocity flows and achieve better performance on the
345 segmentation of glacier ice.

Chapter 2

Physics-Informed LSTM Network For Velocity Prediction of Fluid Flow Simulations

2.1 The Importance of Fluid Flow Velocity Prediction

In fluid flow velocity prediction you model a system that describes some physical geometry and specific fluids with some initial boundary conditions and predict how these fluids will flow and interact in the system and what the fluid velocities will be at every point in the system after a certain amount of time has passed given the initial boundary conditions. This problem is important in mechanical engineering as the mechanical designs of airplane wings, turbines, and other important machinery are based on how they will interact with the flow of air, water, and other particles in the atmosphere or environment where they are used.

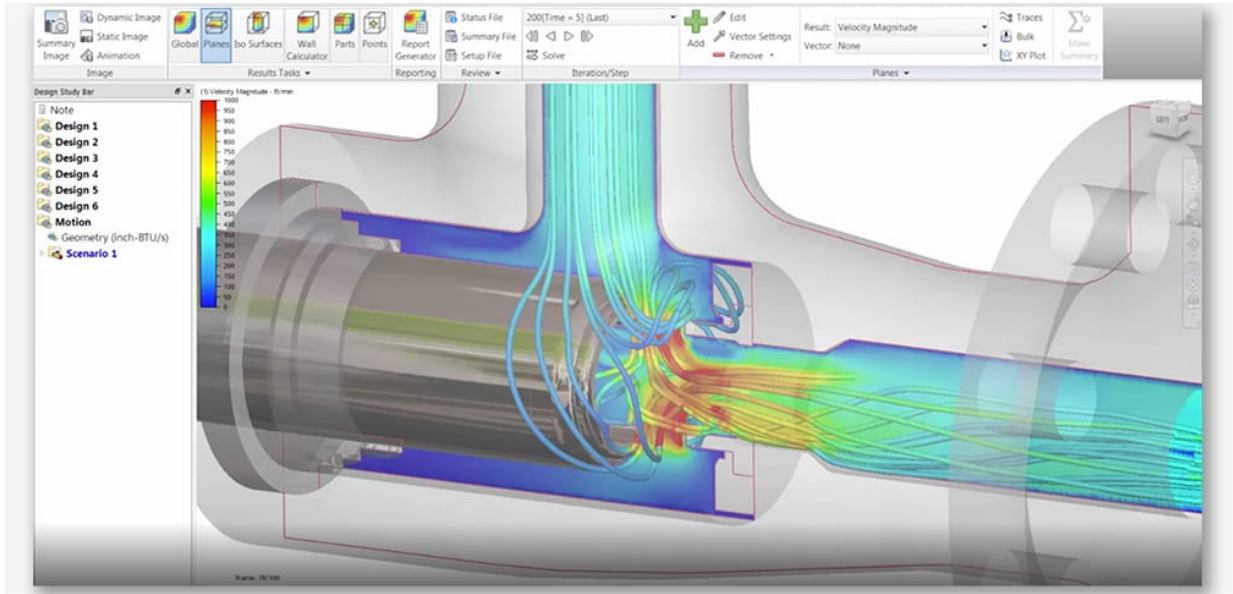


Figure 2.1: An example of a Computational Fluid Dynamics (CFD) simulation predicting the fluid flow velocities in an engine.

359 **2.2 Long Short-Term Memory Networks (LSTMs) For**
 360 **Time Series Data**

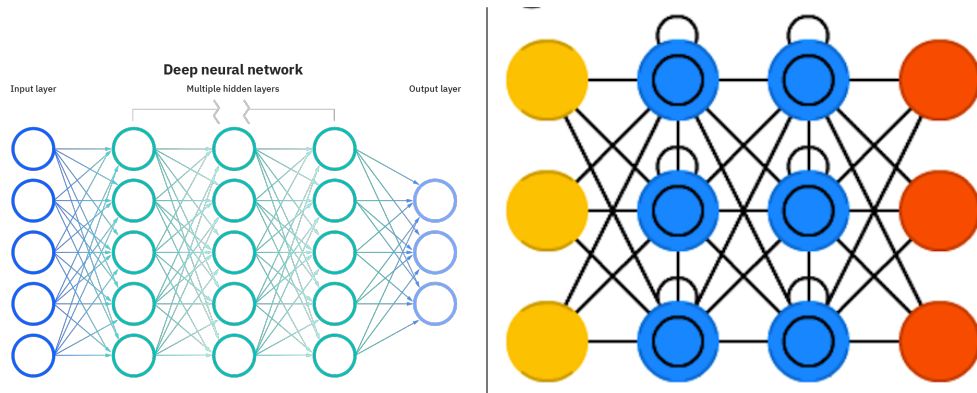


Figure 2.2: A regular 3-layer dense neural network on the left, an LSTM on the right. On the LSTM the blue dots with circles are the specialized LSTM cells, and note how self-connections from RNNs are present in LSTMs as well.

361 Long Short-Term Memory Networks (LSTMs) [21] are neural network models designed to
 362 learn long term dependencies in sequential datasets and are a variation of the Recurrent
 363 Neural Network (RNN). LSTMs selectively pick and store short-term information that
 364 might be useful to know for later using a unique cell structure that includes an input,
 365 forget, and output gate. These gates determine what past information to forget and what
 366 new information to keep track of and it is through this mechanism of storing short memories
 367 for a long period of time where “long” short-term memory derives the name from.

LONG SHORT-TERM MEMORY NEURAL NETWORKS

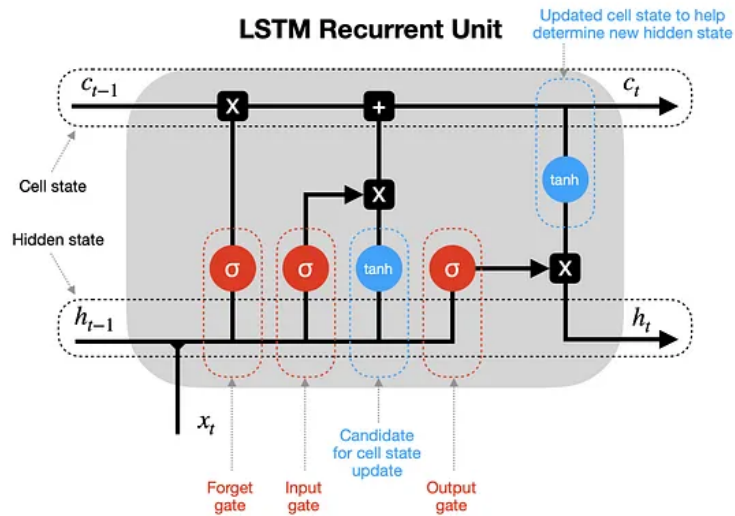


Figure 2.3: An LSTM cell or unit showing all the gates and operations.

368 2.3 Adding Physics to LSTMs

369 I began to tackle the problem of fluid flow predictions by creating a new neural network
 370 architecture based on a combination of Physics-Informed Neural Networks (PINNs) and

371 Long-Short Term Memory Networks (LSTMs) [24]. Specifically, we created a two-branch
372 network architecture that takes as inputs the measurements taken from a Computational
373 Fluid Dynamic (CFD) simulation and predicts what the velocity components (in 2D) will
374 be for a given timestep.

375 **2.3.1 Fluid Flow Velocity Data From Simulations**

376 The data was generated using Ansys by creating a simulation in which we modeled a
377 water-braking scoop mechanism in 2D space, constraining the domain of the model to a
378 2.2 meter by 4 meter box and running the simulation with different inlet velocity profiles.
379 The simulation geometry, mesh, and boundary conditions can be seen in Figures 1.2, 1.1,
380 and 1.3 in the Introduction section.

381 The following figures demonstrate the simulation results for different boundary condi-
382 tions at specific times in the simulation. For the figures with two pictures, the left picture
383 represents the pressure and velocity contours and the right picture the velocity and water
384 volume fraction.

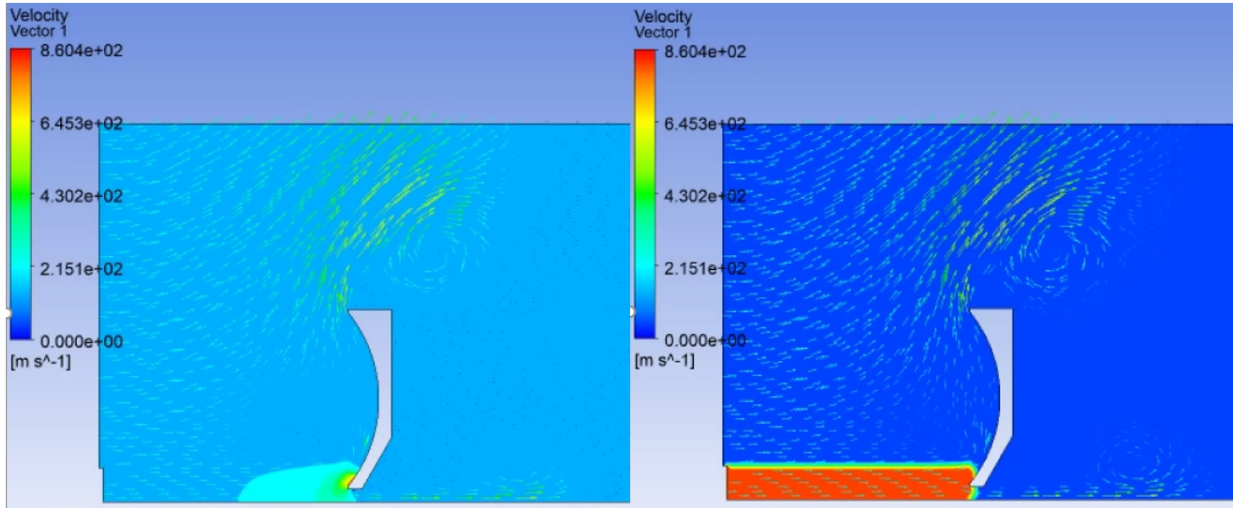


Figure 2.4: Velocity Inlet = 250m/s, Time = 0.011sec

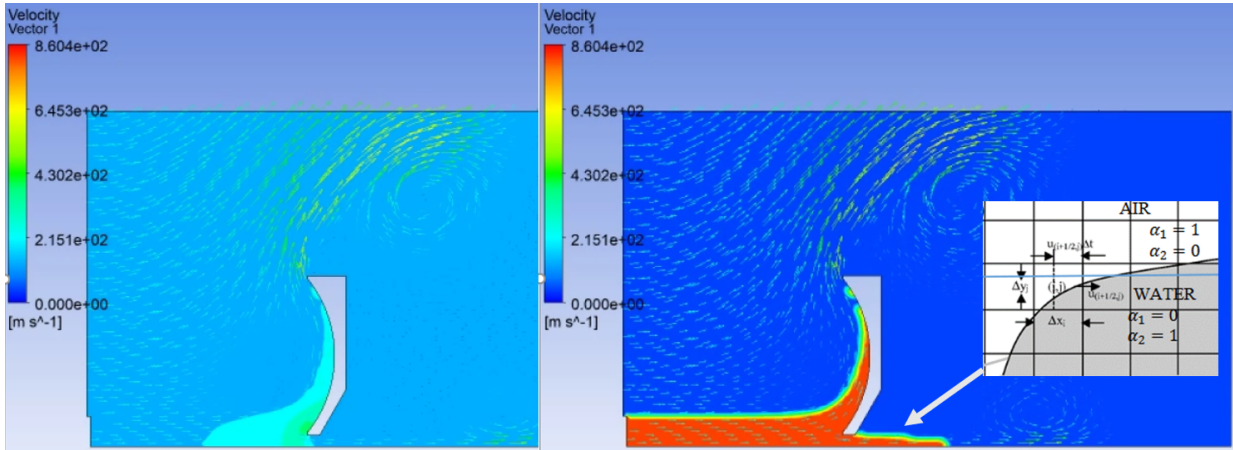


Figure 2.5: Velocity Inlet = 250m/s, Time = 0.016sec.

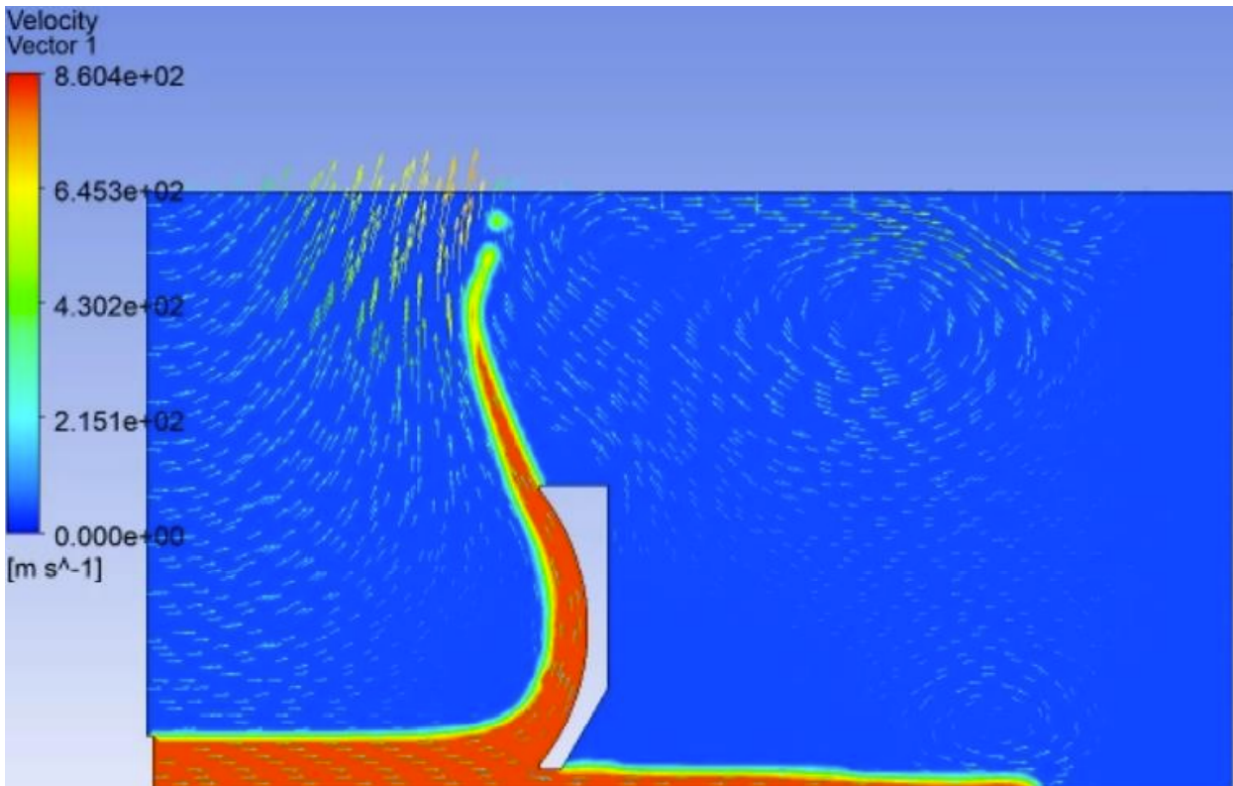


Figure 2.6: Velocity Inlet = 250m/s, Time = 0.025sec

385 The 7 measurements stored for each data sample in the simulation were:

- 386
- The x-coordinate of the node, x

- 387 • The y-coordinate of the node, y
- 388 • The timestep, t
- 389 • The pressure (in atmospheres), p
- 390 • The u-velocity representing the x-component of the velocity field, u
- 391 • The v-velocity representing the y-component of the velocity field, v
- 392 • The water volume fraction or percentage of water from 0 to 1, $w.vf$

393 From now on, we will refer to data samples with the letter x , so for example x^p is the
 394 pressure of the sample x and x_t^p is the pressure of the sample x at a specific point in time
 395 t .

396 2.3.2 Measuring Network Performance With The Mean Squared 397 Error

To measure the performance of our neural network we used a metric called **Mean Squared Error** which computes how erroneous our predictions were on average from the real values. The metric is defined in Equation 2.1 below.

$$\frac{1}{n} \sum_{i=1}^n (y_{pred} - y_{true})^2 \tag{2.1}$$

398 where y_{true} was the real value, y_{pred} was our predicted value, and n was the number of
 399 values or samples we were comparing.

400 For perfect predictions the value of $MSE = 0$. Therefore, the closer to 0 the better a
 401 model is performing.

402 **2.3.3 Proposed Network Architecture**

403 The proposed two-branch neural network took a range of time of measurements as input
 404 called the “lookback” and outputted the velocity components u and v that were predicted
 405 for the same position in space for the next timestep. The LSTM branch incorporated
 406 knowledge about the sequence and the Physics-Informed branch incorporated knowledge
 407 about the Partial Differential Equations (PDEs) describing in-compressible 2D discrete
 408 Navier-Stokes fluid flows. The architecture looked as follows:

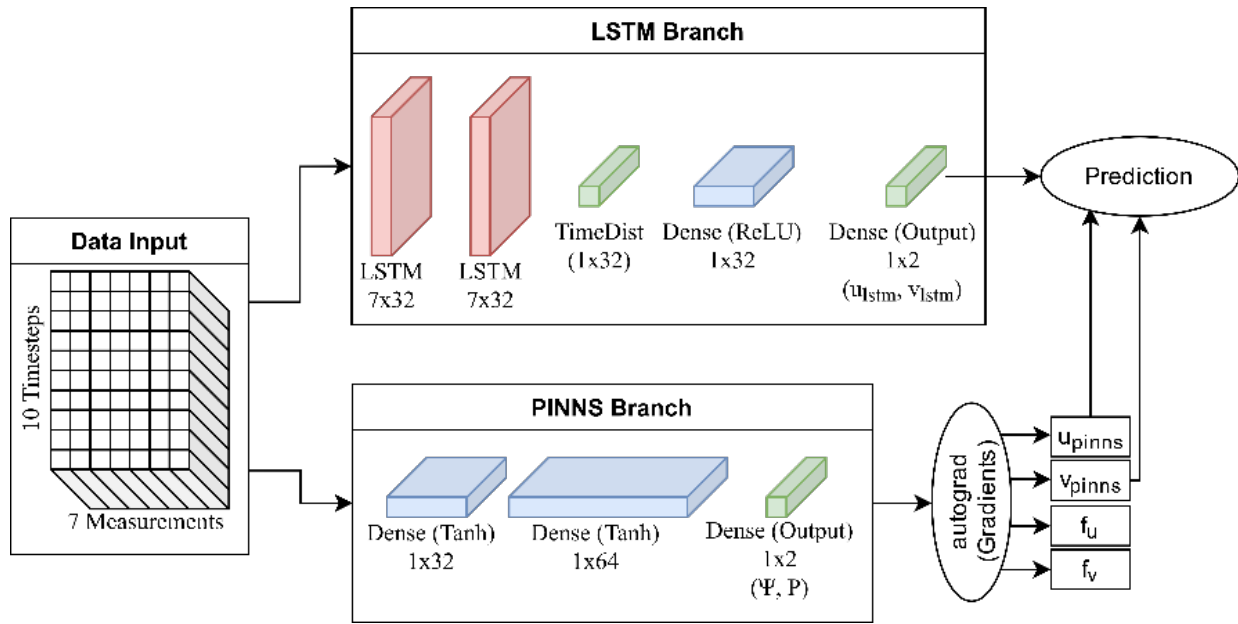


Figure 2.7: Physics-Informed LSTM Architecture showing both the LSTM and Physics-Informed branches and their connection to the final output prediction.

409 **LSTM Branch**

410 The LSTM branch had two stacked bi-directional LSTM layers with 32 activations each,
 411 followed by a Time Distributed layer that used a fully connected layer of 32 activations
 412 with a linear activation function. The Time Distributed layer applied the same weights to
 413 the previous LSTM outputs one timestep at a time. The LSTM layers were followed by a
 414 fully connected layer with 32 activations using the ReLU [25] non-linear activation function

415 which was then followed by a fully connected output layer. The output layer consisted of
 416 two outputs, the x-component of the velocity field called u which was represented as u_{lstm}
 417 and the y-component of the velocity field called v which was represented as v_{lstm} . The
 418 LSTM layers were connected to the fully connected part of the network by concatenating
 419 the two directional hidden states outputted by the last LSTM layer.

420 **Physics-Informed Branch**

421 As described in [18], the general 2D Navier-Stokes equations:

$$\begin{aligned}
 u_t + p_x + \lambda_1(uu_x + vu_y) - \lambda_2(u_{xx} + u_{yy}) &= 0 \\
 v_t + p_y + \lambda_1(uv_x + vv_y) - \lambda_2(v_{xx} + v_{yy}) &= 0 \\
 u_x + v_y &= 0
 \end{aligned}
 \tag{2.2}$$

422 We assumed that for some latent function $\psi(x, y, t)$

$$\begin{aligned}
 u &= \psi_y \\
 v &= -\psi_x
 \end{aligned}
 \tag{2.3}$$

423 Then we approximated $\psi(x, y, t)$ using a dense neural network f with three inputs
 424 (x, y, t) , two outputs (u, v) , and two learnable parameters (λ_1, λ_2) .

$$\begin{aligned}
 f_u(x, y, t) &:= u_t + p_x + \lambda_1(uu_x + vu_y) - \lambda_2(u_{xx} + u_{yy}) \\
 f_v(x, y, t) &:= v_t + p_y + \lambda_1(uv_x + vv_y) - \lambda_2(v_{xx} + v_{yy})
 \end{aligned}
 \tag{2.4}$$

The combined physics loss we needed to minimize was then computed from the following

four losses:

$$\begin{aligned}
 MSE_u &= \frac{1}{n} \sum_{i=1}^n (\psi_y - u^i)^2 \\
 MSE_v &= \frac{1}{n} \sum_{i=1}^n (-\psi_x - v^i)^2 \\
 MSE_{f_u} &= \frac{1}{n} \sum_{i=1}^n (f_u(x^i, y^i, t^i))^2 \\
 MSE_{f_v} &= \frac{1}{n} \sum_{i=1}^n (f_v(x^i, y^i, t^i))^2
 \end{aligned}
 \tag{2.5}$$

425 Such that the total loss was:

$$MSE_{total} = MSE_u + MSE_v + MSE_{f_u} + MSE_{f_v}
 \tag{2.6}$$

426 The architecture consisted of a simple dense network with 3 layers. The first layer had 32
 427 activations and used the hyperbolic tangent non-linear activation function (tanh), followed
 428 by another fully connected layer with 64 activations using tanh once again, followed by the
 429 output layer with two outputs. The automatic differentiation system included in PyTorch
 430 named **autograd** was used to compute the partial derivatives required for the computation
 431 of the final physics loss.

432 **Two-Branch Combined Model**

433 The two outputs of each branch were combined by using a weight α that was set between
 434 0 and 1. For our experiments, $\alpha = 0.5$ (but in the future it could be set as a learnable
 435 parameter)

$$\begin{aligned}
 u_{pred} &= \alpha * u_{lstm} + (1 - \alpha) * u_{pinns} \\
 v_{pred} &= \alpha * v_{lstm} + (1 - \alpha) * v_{pinns}
 \end{aligned}
 \tag{2.7}$$

436 where (u_{pred}, v_{pred}) were the final predictions, (u_{lstm}, v_{lstm}) were the two outputs of the
 437 LSTM branch, and (u_{pinns}, v_{pinns}) were the two outputs of the Physics-Informed branch.

438 2.3.4 Baseline Used To Compare Against Our Proposed Network

439 The baseline used for this model was to simply assume that the velocities at the next
 440 timestep will be the same as those in the previous timestep for each data point.

$$\begin{aligned}
 prev_u &= x_t^u \\
 prev_v &= x_t^v \\
 y_{t+1}^{pred} &= (prev_u, prev_v)
 \end{aligned}
 \tag{2.8}$$

441 where t was the current timestep, x_t was the current data sample, x_t^u was the u-velocity
 442 component of x_t , x_t^v was the v-velocity component of x_t , and y_{t+1}^{pred} was our predicted velocity.

443 2.3.5 Experimental Results

444 The following table summarizes the results of the experiments and provides the mean
 445 squared error for the velocity components \mathbf{U} and \mathbf{V} for each model along with the total
 446 training time after 200 epochs. The experiments were performed using an NVIDIA RTX
 447 3090 and every epoch took around 27 seconds for non-informed LSTM models and 30
 448 seconds for physics-informed LSTM models.

Model	U	V	Time (min)
Baseline	5.455	2.561	0.061
PINNS Only	5709	12038	80
LSTM Only	1.7811	8.6962	117
PINNS+LSTM	0.4677	1.2794	142

Table 2.1: Comparison of the performance (MSE) of different models when using the 250m/s simulation for training and the 300m/s simulation for testing.

449 **2.3.6 Conclusion**

450 Our experimental results in Table 2.1 show that the Physics-Informed LSTM outperforms
451 the non-informed LSTM approach and leads us to our conclusion that informing the LSTM
452 about the governing physics leads to better performance than just using LSTMs or PINNs
453 by themselves.

Chapter 3

Glacial Ice Segmentation of the HKH Region With Physics-Informed Data Augmentation

3.1 The Importance of Glacial Ice Segmentation

Glacial ice segmentation refers to the problem of gathering hyperspectral images taken by satellites of different glaciers and segmenting or delineating which areas are glacial ice, which areas are debris covered ice (ice mixed with rocks), and which areas are just rocks. This problem is important in the field of geology as monitoring the amount and location of ice from glaciers such as the ones in the Hindu Kush Himalayas (HKH) is critical as these glaciers provide a source of freshwater to a big population of the world.

3.2 Image Semantic Segmentation: Grouping Similar Pixels Together

The task of semantic segmentation refers to grouping similar or related pixels of an image together, like those of a specific object. For example, grouping all the pixels of people, roads, buildings, or trees as seen in the figure below:







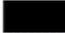
 Road	 Sidewalk	 Building	 Fence
 Pole	 Vegetation	 Vehicle	 Unlabel

Figure 3.1: An example of semantic segmentation of an image. The pixels are grouped together by different categories.

470 **3.3 Glacier Mapping Through Segmentation of Ice in**
471 **Hyperspectral Images**

472 Glacial ice segmentation or glacier mapping is simply the task of semantic segmentation
473 applied to hyperspectral satellite images of glaciers. The goal is to determine for each pixel
474 in the image whether the pixel is an area of glacial ice, debris covered ice, or background
475 (regular rocks) as shown in the figure below:

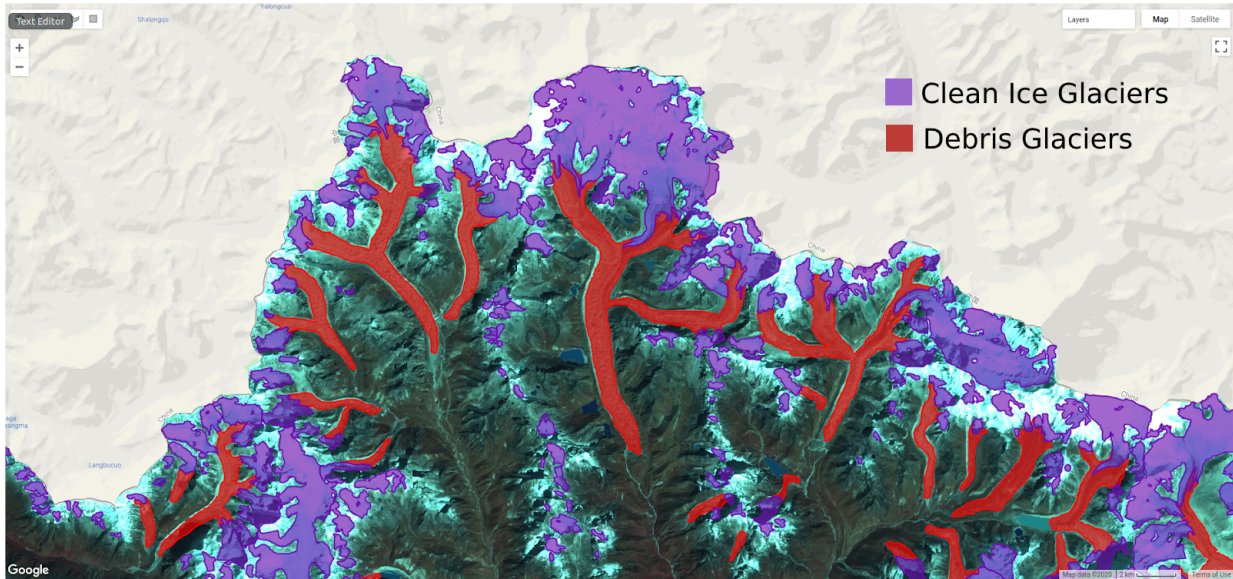


Figure 3.2: Semantic segmentation of a glacier satellite image by a human annotator.

3.4 Convolutional Neural Networks: The Backbone of Almost All Networks That Use Images

Convolutional Neural Networks [26] are one of the most important and fundamental neural network models when dealing with datasets that contain images and their role in state-of-the-art architectures in image classification competitions such as ImageNet and other image tasks cannot be understated. CNNs operate by assuming the inputs are images and performing operations on the pixels of these images called convolutions. The purpose of these convolution operations is to apply a ‘filter’ to extract important features out of these images as feature maps, and because these CNNs are neural networks these ‘filters’ or ‘kernels’ automatically learn to filter out information which might be useful for the specific task we are trying to solve. After the convolution operations a pooling operation is applied to the extracted feature maps which reduces size of these maps and the computational complexity of the network. A common pooling operation is ‘2x2 max-pooling’ where the image is split into 2x2 patches and the maximum value at each of these patches is used to

490 create the new reduced size feature map, the idea being that the most prominent features or
 491 those with high values are the most important for solving image problems. After extracting
 492 important features of images through convolutions and pooling layers the next step in CNNs
 493 is to convert the 2D feature maps into 1D vectors by flattening them out and then feeding
 494 these feature vectors as inputs to a regular dense network to get a final output. The layers
 495 of this dense network are typically called ‘fully-connected layers’ to differentiate them from
 496 the ‘convolutional layers’.

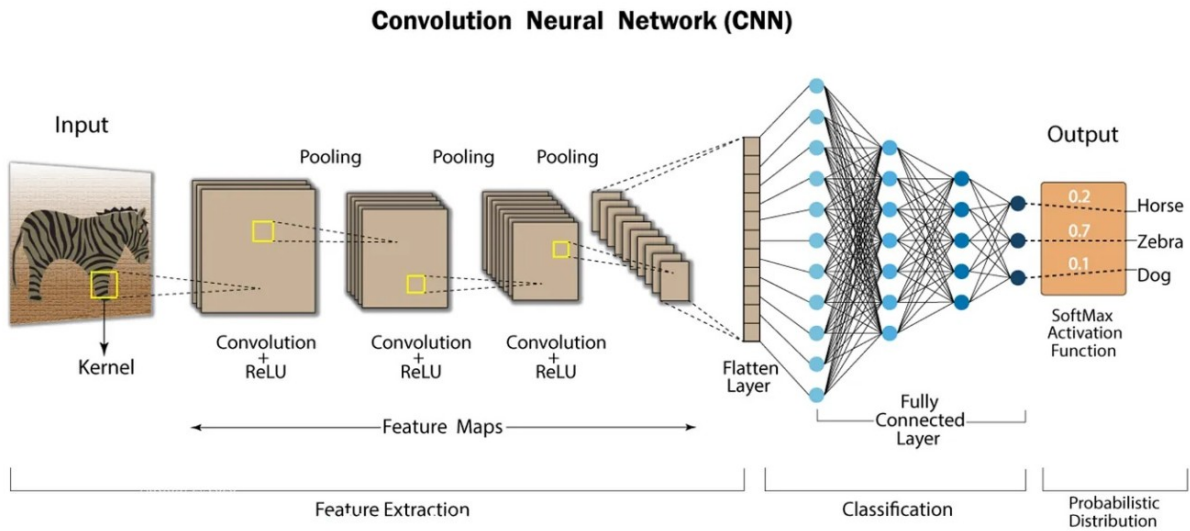


Figure 3.3: An example of a CNN model for an animal classification problem. Features are extracted with convolutions and pooling, and then used in a fully connected network for a final classification.

497 **3.5 UNet: The Standard Network For Image Segmen-** 498 **tation**

499 U-Net [27] is a variation of a CNN and was derived from the improvements achieved by
 500 Fully Connected Convolutional Networks (FCNs) for semantic segmentation [28]. FCNs
 501 transform the fully-connected layers of a CNN into convolutional layers and through an
 502 upsampling strategy called ‘deconvolution’ or ‘transposed convolution’ output an image

503 that is the same size as the original image. U-Net is split into two components, and
 504 encoder in the left half of the U-shape and a decoder in the right half.

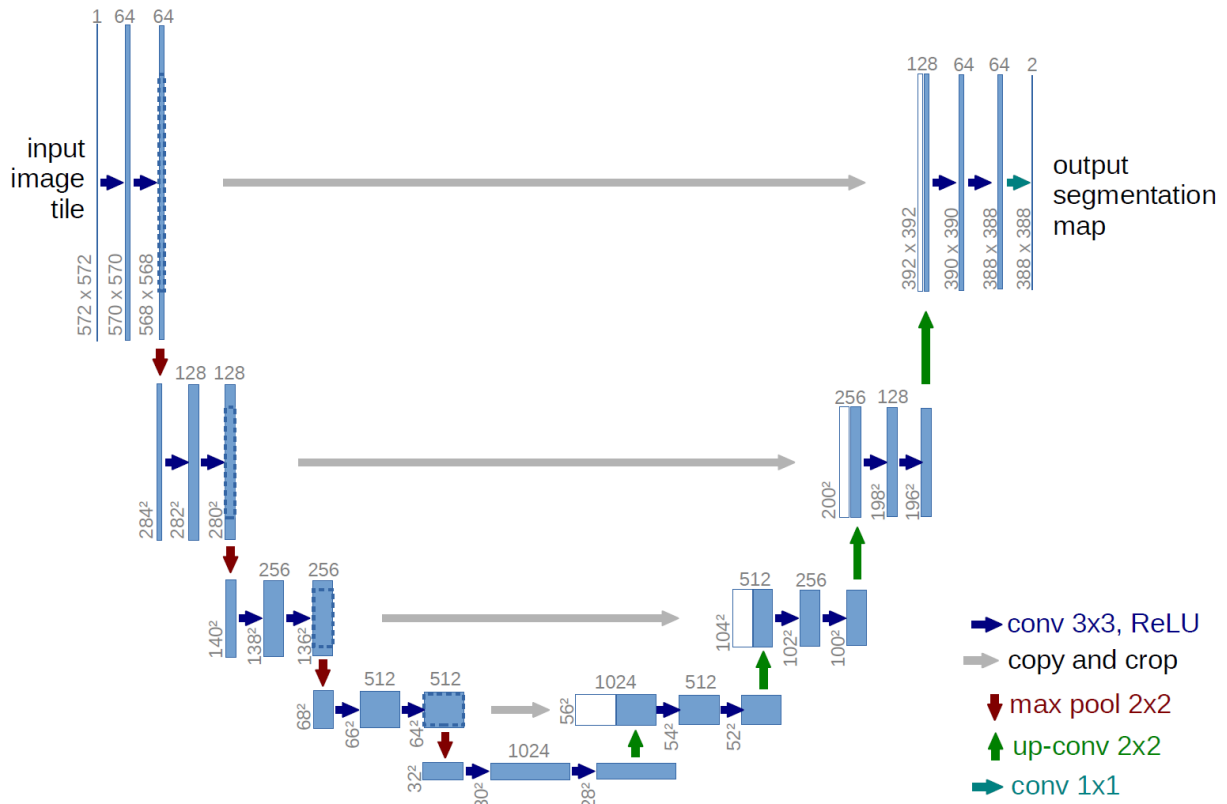


Figure 3.4: U-Net architecture showing both components and how they are connected to output a final segmentation map. Note the straight connections feeding previous inputs into later outputs going straight across.

505 The encoder also known as the contracting path is the left half of the U-shape that
 506 takes the original input image, applies regular convolutions and max-pooling, and outputs
 507 a reduced size feature map at the bottom. This is the feature extraction component that
 508 aims to capture the important context of the image.

509 The decoder also known as the expanding path is the right half of the U-shape that
 510 takes the feature map from the encoder and through ‘transposed convolutions’ or ‘up-
 511 convolutions’ upsamples and expands the feature map all the way until we get an output
 512 segmentation map which is the same size as the original input image.

513 Lastly, to help the decoder maintain some of the location information that is lost while
514 encoding there are ‘skip-connections’ going from the encoder to the decoder straight across
515 the U-shape.

516 U-Net achieved state-of-the-art results when introduced in 2015 for biomedical image
517 segmentation and these types of networks are still used to this day for many segmentation
518 problems as a starting baseline.

519 3.5.1 Measuring Network Performance With IoU

520 To measure the performance of the segmentation model, the main metric we used was the
521 **Intersection over Union (IoU)** which is defined in Figure 3.5 below and has numbers
522 in the range from 0 to 1 with 1 being a perfect score.

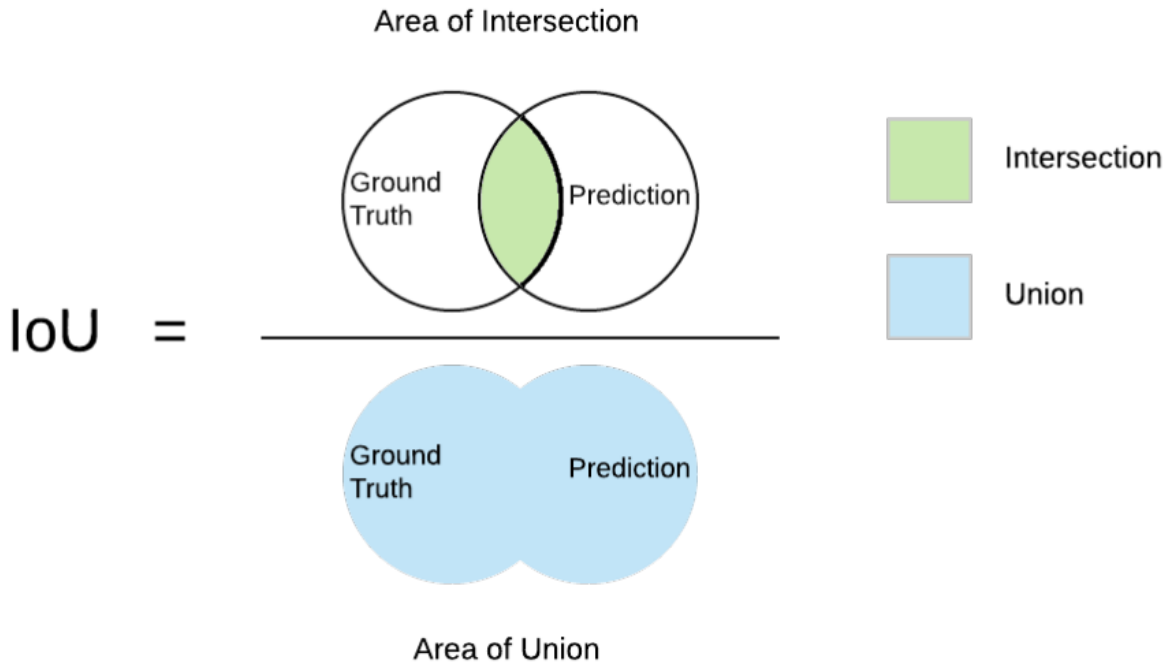


Figure 3.5: Definition of Intersection over Union.



Figure 3.6: Three examples of different IoU values and what type of performance they represent.

3.6 Adding Physics To Image Segmentation Through Data Augmentation

As a first step towards tackling the problem of glacial ice segmentation I began by taking a previously proposed architecture for segmentation of the Hindu Kush Himalayas (HKH) region glaciers [22] and improving its performance by adding physics to the model through data augmentation.

The main idea was to take the elevation map from the satellite images and encode an abstract representation of a “precipitation model” from that elevation map as a new channel of the image. Although the actual physics equations of ice flow were not explicitly encoded in this new data channel, this new data was created from an abstract representation of the physics and we therefore called it a physics-informed data augmentation. In this channel we simulated precipitation and encoded paths where water or ice might flow from the top to the valley of the glaciers.

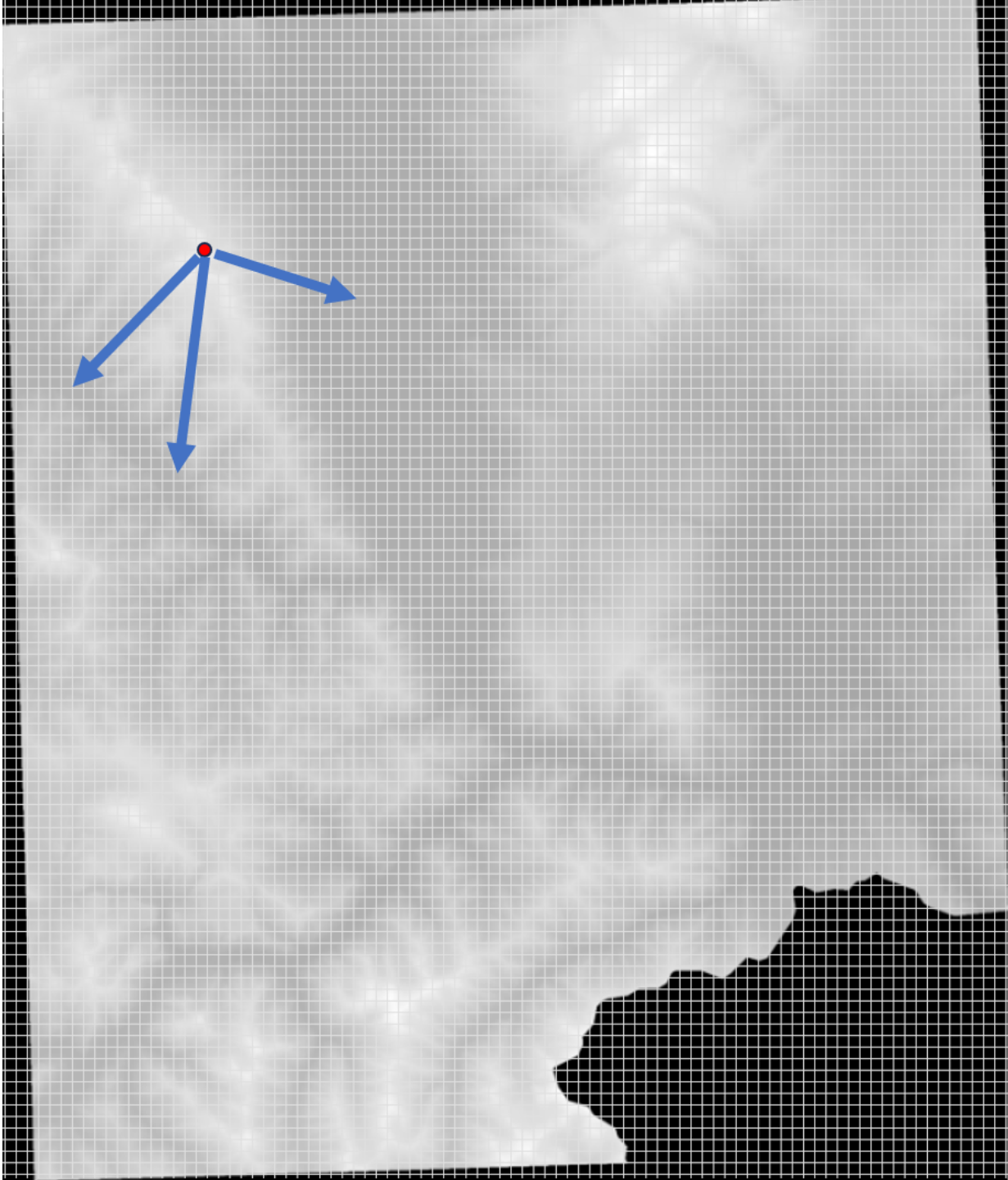


Figure 3.7: For each pixel in the image we simulated precipitation going down the glacier and accumulating, then we encoded such information as an additional physics-informed channel.

536 Specifically, the algorithm as follows:

- 537 1. Take the elevation map as the input image *elevation*
- 538 2. Create an empty image of the same size as the input called *output*
- 539 3. For each pixel in the image, perform Breadth-First Search (BFS) with a special
540 limitation where you can only visit pixels you haven't visited before AND that are
541 lower elevation than the current pixel popped from the queue as water/ice can only
542 flow down.
- 543 4. Each time a pixel is visited, the *output* at that pixel's position increases by 1 as 1
544 drop of water/ice has flowed down to it.
- 545 5. At the end, normalize the image between 0 and 1 by subtracting the mean and
546 dividing by the standard deviation.

547 In pseudocode, the data augmentation algorithm would look like:

Algorithm 1 Physics-Informed Data Augmentation Algorithm

```
im ← elevation map from satellite image
output ← image full of zeros the same size as im
im.shape[0] ← number of rows in im
im.shape[1] ← number of columns in im
for u := 0 → im.shape[0] do
  for v := 0 → im.shape[1] do
    Breadth_First_Search(im, output, u, v)
  end for
end for
im = (im - im.mean())/im.std()
```

548 With the modified BFS algorithm being:

Algorithm 2 Physics-Informed Breadth-First Search

```
im ← elevation map from satellite image
output ← previous accumulated output from other pixels
u ← row of source pixel
v ← column of source pixel
source ← (u, v)
visited = source
Q = Queue with source appended to it
while Q ≠ Empty do
    x = Q.pop()
    curr_elevation ← im[x]
    if x ≠ source then
        output[x] + = 1
    end if
    for n in get_neighbors(im, x) do
        n_elevation ← im[n]
        if n not visited & n_elevation < curr_elevation then
            Add n to visited
            Append n to Q
        end if
    end for
end while
```

549 The following figure presents an example of the results after performing the augmenta-
550 tion.

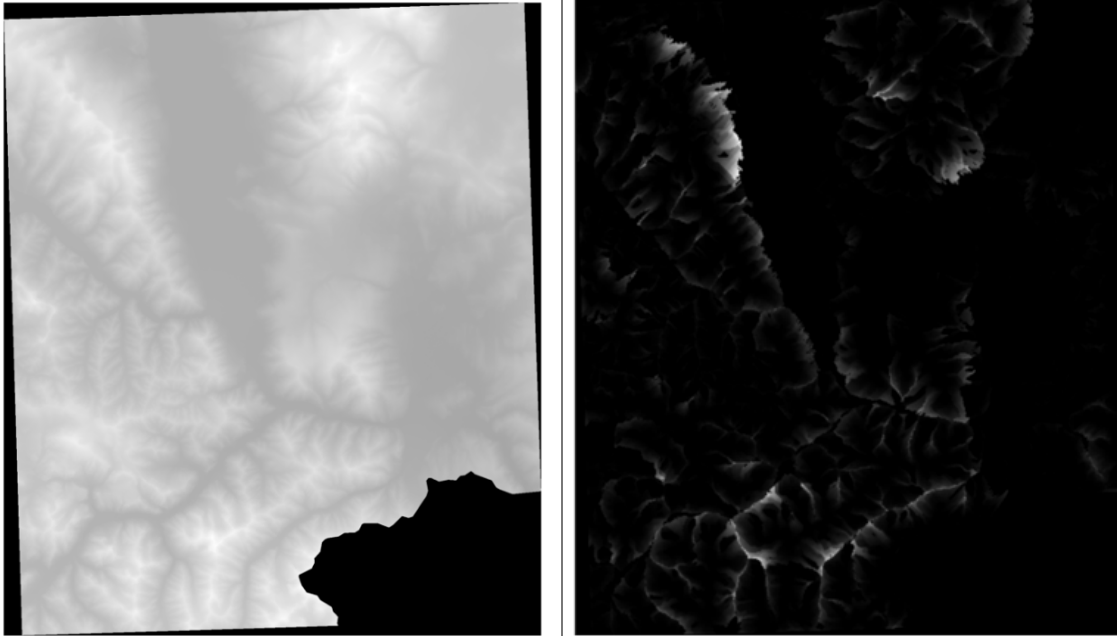


Figure 3.8: Left is the elevation map from one of the glacier satellite images where white pixels are peaks and darker pixels are valleys. Right is the resulting physics-informed data augmentation channel.

551 **3.6.1 Glacier Mapping Data From ICIMOD And Landsat7 Satel-**
 552 **lite**

553 The data used to train and evaluate the models were gathered and labelled by experts at the
 554 International Centre for Integrated Mountain Development (ICIMOD) from multispectral
 555 imagery from NASA’s Landsat 7 satellite for the glaciers of the Hindu Kush Himalayas
 556 region from 2002 to 2008.

557 **3.6.2 Baseline Network**

558 The baseline model used to evaluate our proposed data augmentation technique was the
 559 Boundary-Aware U-Net for Glacier Segmentation model developed and published in 2023 by
 560 Bibek et. al [22]. No modifications to the model were made apart from slight changes to the
 561 hyperparameter configuration and the addition of the physics-informed data augmentation

562 technique.

563 3.6.3 Experimental Results

Model	Background IoU	CleanIce IoU	DebrisIce IoU
Regular U-Net	N/A	N/A	0.2850
Regular U-Net	N/A	0.6560	N/A
Boundary-Aware U-Net (Baseline)	N/A	N/A	0.3594
Boundary-Aware U-Net (Baseline)	N/A	0.6817	N/A
Physics & Boundary-Aware U-Net (mine)	0.8640	0.6350	0.3850

Table 3.1: Comparison of the performance of different neural network models by the Intersection Over the Union (IoU) between the predicted labels and the true labels for each class. IoU is a metric between 0 and 1, with 1 being a perfect score.

564 3.6.4 Conclusion

565 The current experimental results demonstrate that my proposed physics-informed data
566 augmentation leads to improved performance for the segmentation of Debris-covered Ice
567 from the baseline model. This is significant as classification of Debris-covered Ice is a more
568 challenging task than that of Clean Ice for both the baseline model and expert glaciologists.
569 With some hyper-parameter tuning I hypothesize that we can reach up to 0.40 IoU, and by
570 switching U-Net to a newer state-of-the-art segmentation model such as MANet [29] along
571 with using newer loss functions such as the Unified Focal Loss [30] I believe we might be able
572 to reach above 0.50 IoU. Although my proposed approach does not outperform the baseline
573 for Clean Ice segmentation, I believe this is due to the fact that the original baseline uses
574 two separate binary models for segmentation of each class instead of one unified multi-class
575 model. I will train two separate binary models for a more fair comparison in the final
576 version of my full dissertation.

Chapter 4

577

Physics-Informed Network For Glacial Ice Velocity Predictions

578

579

580 As my next step, I propose making a new Physics-Informed architecture based on what I
581 learned from the Physics-Informed LSTM Network [24] which I previously applied to fluid
582 flow simulations and adapting it to the problem of glacial ice velocity prediction. Glacial
583 ice velocity prediction is simply the problem of fluid flow velocity prediction where the fluid
584 is ice from a glacier. The aim of this step is to prepare a network architecture and dataset
585 than can be later incorporated into the glacier segmentation problem as I hypothesize that
586 including velocity information based on the physics laws of fluid flow will improve the
587 performance of the glacier segmentation models proposed by [22]. There already exists a
588 dataset of glacier ice velocities [31] for satellite images created by the National Snow and Ice
589 Data Center which can be easily adapted and incorporated with my previous methodology
590 for velocity predictions. However, since then I have learned about newer architectures that
591 perform better than LSTMs [21] such as GRUs [32] and Transformers [33] which I would
592 like to try as well.

593 The main challenge with this step is determining how to set-up the Physics-Informed
594 part of the network as my previous work focused on air and water flows and not ice flows.
595 The architecture will not require many changes, it is the loss function which was based
596 on the incompressible 2D Navier-Stokes equations which might need to be modified to
597 accommodate the new type of data.

Chapter 5

598

599 **Physics-Informed MANet for Glacial** 600 **Ice Segmentation of the HKH Region**

601 As my final step, I propose combining the Physics-Informed Network used for velocity pre-
602 diction and the U-Net used for image segmentation to further improve the performance on
603 the segmentation of ice in the HKH region. I will do this by trying two different method-
604 ologies. In the first methodology, I will simply create a two branch network the same way
605 I did with the Physics-Informed + LSTM network where we just have to carefully connect
606 the inputs and outputs of their respective branches correctly. In the second methodology,
607 I will use a self-learning loss that will combine the losses of both networks into one and
608 optimize them both at the same time. The self-learning combined loss will be as follows:

$$L_{Combined} = \alpha * L_{UNET} + (1 - \alpha) * L_{PINNS} \quad (5.1)$$

609 where $L_{Combined}$ is the new combined loss from both networks, L_{UNET} is the loss of the
610 UNet ice segmentation network and L_{PINNS} is the loss of the Physics-Informed velocity
611 prediction network. This loss is based on the self-learning boundary aware loss specified in
612 [22].

613 The main challenge will be combining the datasets for the combined network as they
614 were not taken at the same exact time and so the satellite images used for segmentation
615 and the velocity images are slightly different. I do not believe this will present a major
616 problem, as I have the script used to get both datasets so I will be able to control how
617 far apart these datasets are in real time to minimize the error introduced by this problem.

618 I will also try a newer segmentation architecture that has been shown to be better than
619 UNet called MANet [29] which I hypothesize will give me the best performance in the end.

620 Lastly, I will develop a simple WebUI that allows glaciologists to feed their own hy-
621 perspectral satellite images to our trained models to get labeled masks of glacial ice in a
622 format that can be loaded into QGIS to help them with their glacier mapping efforts.

Bibliography

623

- 624 1. Rombach R, Blattmann A, Lorenz D, Esser P, and Ommer B. High-Resolution Image
625 Synthesis with Latent Diffusion Models. 2022 IEEE/CVF Conference on Computer
626 Vision and Pattern Recognition (CVPR) 2021:10674–85.
- 627 2. Redmon J, Divvala SK, Girshick RB, and Farhadi A. You Only Look Once: Unified,
628 Real-Time Object Detection. 2016 IEEE Conference on Computer Vision and Pattern
629 Recognition (CVPR) 2015:779–88.
- 630 3. Tan M and Le QV. EfficientNet: Rethinking Model Scaling for Convolutional Neural
631 Networks. ArXiv 2019;abs/1905.11946.
- 632 4. Devlin J, Chang MW, Lee K, and Toutanova K. BERT: Pre-training of Deep Bidirec-
633 tional Transformers for Language Understanding. In: *North American Chapter of the*
634 *Association for Computational Linguistics*. 2019. URL: <https://api.semanticscholar.org/CorpusID:52967399>.
- 635 5. Brown TB, Mann B, Ryder N, et al. Language Models are Few-Shot Learners. ArXiv
636 2020;abs/2005.14165.
- 637 6. Amankwa G. Modeling the Spatiotemporal Dynamics of Active Regions on the Sun
638 Using Deep Neural Networks. PhD thesis. University of Texas, El Paso, 2021.
- 639 7. Mao J, Shi S, Wang X, and Li H. 3D Object Detection for Autonomous Driving: A
640 Comprehensive Survey. *International Journal of Computer Vision* 2022;131:1909–63.
- 641 8. Tolstikhin IO, Houlsby N, Kolesnikov A, et al. MLP-Mixer: An all-MLP Architecture
642 for Vision. ArXiv 2021;abs/2105.01601.
- 643 9. Karras T, Laine S, Aittala M, Hellsten J, Lehtinen J, and Aila T. Analyzing and
644 Improving the Image Quality of StyleGAN. 2020 IEEE/CVF Conference on Computer
645 Vision and Pattern Recognition (CVPR) 2019:8107–16.
- 646

- 647 10. Deng J, Dong W, Socher R, Li LJ, Li K, and Fei-Fei L. ImageNet: A large-scale
648 hierarchical image database. 2009 IEEE Conference on Computer Vision and Pattern
649 Recognition 2009:248–55.
- 650 11. Lin TY, Maire M, Belongie SJ, et al. Microsoft COCO: Common Objects in Con-
651 text. In: *European Conference on Computer Vision*. 2014. URL: [https://api .
652 semanticscholar.org/CorpusID:14113767](https://api.semanticscholar.org/CorpusID:14113767).
- 653 12. Karras T, Laine S, and Aila T. A Style-Based Generator Architecture for Generative
654 Adversarial Networks. 2019 IEEE/CVF Conference on Computer Vision and Pattern
655 Recognition (CVPR) 2018:4396–405.
- 656 13. Deng L. The MNIST database of handwritten digit images for machine learning re-
657 search. *IEEE Signal Processing Magazine* 2012;29:141–2.
- 658 14. Finn C, Abbeel P, and Levine S. Model-Agnostic Meta-Learning for Fast Adaptation
659 of Deep Networks. In: *International Conference on Machine Learning*. 2017. URL:
660 <https://api.semanticscholar.org/CorpusID:6719686>.
- 661 15. Koch GR. Siamese Neural Networks for One-Shot Image Recognition. In: 2015. URL:
662 <https://api.semanticscholar.org/CorpusID:13874643>.
- 663 16. Snell J, Swersky K, and Zemel RS. Prototypical Networks for Few-shot Learning. In:
664 *Neural Information Processing Systems*. 2017. URL: [https://api.semanticscholar .
665 org/CorpusID:309759](https://api.semanticscholar.org/CorpusID:309759).
- 666 17. Sung F, Yang Y, Zhang L, Xiang T, Torr PHS, and Hospedales TM. Learning to
667 Compare: Relation Network for Few-Shot Learning. 2018 IEEE/CVF Conference on
668 Computer Vision and Pattern Recognition 2017:1199–208.
- 669 18. Raissi M, Perdikaris P, and Karniadakis GE. Physics-informed neural networks: A
670 deep learning framework for solving forward and inverse problems involving nonlinear
671 partial differential equations. *J. Comput. Phys.* 2019;378:686–707.
- 672 19. ANSYS Fluent. Canonsburg, PA.

- 673 20. National Snow and Ice Data Center. Why Glaciers Matter — National Snow and Ice
674 Data Center. 2023. URL: [https://nsidc.org/learn/parts-cryosphere/glaciers/
675 why-glaciers-matter](https://nsidc.org/learn/parts-cryosphere/glaciers/why-glaciers-matter).
- 676 21. Hochreiter S and Schmidhuber J. Long Short-Term Memory. *Neural Computation*
677 1997;9:1735–80.
- 678 22. Aryal B, Miles K, Vargas Zesati S, and Fuentes O. Boundary Aware U-Net for Glacier
679 Segmentation. In: *Proceedings of the Northern Lights Deep Learning Workshop*. Vol. 4.
680 2023. DOI: 10.7557/18.6789.
- 681 23. Vaswani A, Shazeer N, Parmar N, et al. Attention is All you Need. In: *Advances in*
682 *Neural Information Processing Systems*. Ed. by Guyon I, Luxburg UV, Bengio S, et
683 al. Vol. 30. Curran Associates, Inc., 2017. URL: [https://proceedings.neurips.
684 cc/paper_files/paper/2017/file/3f5ee243547dee91fbd053c1c4a845aa-Paper.
685 pdf](https://proceedings.neurips.cc/paper_files/paper/2017/file/3f5ee243547dee91fbd053c1c4a845aa-Paper.pdf).
- 686 24. Pérez J, Baez R, Terrazas J, et al. Physics-Informed Long-Short Term Memory Neural
687 Network Performance on Holloman High-Speed Test Track Sled Study. *American*
688 *Society of Mechanical Engineers, Fluids Engineering Division (Publication) FEDSM*
689 2022;2.
- 690 25. Fukushima K. Visual Feature Extraction by a Multilayered Network of Analog Thresh-
691 old Elements. *IEEE Trans. Syst. Sci. Cybern.* 1969;5:322–33.
- 692 26. Krizhevsky A, Sutskever I, and Hinton GE. ImageNet classification with deep convo-
693 lutional neural networks. *Communications of the ACM* 2012;60:84–90.
- 694 27. Ronneberger O, Fischer P, and Brox T. U-Net: Convolutional Networks for Biomedical
695 Image Segmentation. *ArXiv* 2015;abs/1505.04597.
- 696 28. Shelhamer E, Long J, and Darrell T. Fully convolutional networks for semantic seg-
697 mentation. 2015 *IEEE Conference on Computer Vision and Pattern Recognition*
698 (CVPR) 2014:3431–40.

- 699 29. Li R, Zheng S, Duan C, and Su J. Multiattention Network for Semantic Segmentation
700 of Fine-Resolution Remote Sensing Images. *IEEE Transactions on Geoscience and*
701 *Remote Sensing* 2020;60:1–13.
- 702 30. Yeung M, Sala E, Schönlieb CB, and Rundo L. Unified Focal loss: Generalising Dice
703 and cross entropy-based losses to handle class imbalanced medical image segmentation.
704 *Computerized Medical Imaging and Graphics* 2022;95:102026.
- 705 31. Fahnestock M, Scambos T, Moon T, Gardner A, Haran T, and Klinger M. Rapid
706 large-area mapping of ice flow using Landsat 8. *Remote Sensing of Environment*
707 2016;185:84–94.
- 708 32. Cho K, Merrienboer B van, Gülçehre Ç, et al. Learning Phrase Representations using
709 RNN Encoder–Decoder for Statistical Machine Translation. In: *Conference on Empiri-*
710 *cal Methods in Natural Language Processing*. 2014. URL: [https://api.semanticscholar.](https://api.semanticscholar.org/CorpusID:5590763)
711 [org/CorpusID:5590763](https://api.semanticscholar.org/CorpusID:5590763).
- 712 33. Dosovitskiy A, Beyer L, Kolesnikov A, et al. An Image is Worth 16x16 Words: Trans-
713 formers for Image Recognition at Scale. *ArXiv* 2020;abs/2010.11929.